ИНСТИТУТ ЯДЕРНОЙ ФИЗИКИ
СО АН СССР

P.M.Ivanov, L.M.Kurdadze, M.Yu.Lelchuk,
V.A.Sidorov, A.N.Skrinsky, A.G.Chilingarov,
Yu.M.Shatunov, B.A.Shwartz, S.I.Eidelman

MEASUREMENT OF CHARGED KAON FORMFACTOR IN THE ENERGY REGION 1.12-1.40 GeV

ПРЕПРИНТ ИЯФ 79-68

Новосибирск

MEASUREMENT OF CHARGED KAON FORMFACTOR IN THE ENERGY REGION 1.12-1.40 GeV

P.M.Ivanov, L.M.Kurdadze, M.Yu.Lelchuk, V.A.Sidorov, A.N.Skrinsky, A.G.Chilingarov, Yu.M.Shatunov, B.A.Shwartz, S.I.Eidelman

Institute of Nuclear Physics
630090, Novosibirsk 90, USSR

Abstract

The cross-section of the reaction $e^+e^- \to K^+K^-$ has been measured at the electron-positron storage ring VEPP-2M at c.m. energy region 1.12-1.40 GeV. The integrated luminosity was 564 nb^{-1}, 1375 K^+K^- events have been selected. Experimental values of the charged kaon formfactor exceed considerably the calculations based on ρ, ω, ϕ resonances.

Submitted to the International Symposium on Lepton and Photon Interactions, Batavia, USA, 1979.

This work is devoted to the measurement of $e^+e^- \to K^+K^+$ cross-section. The data have been obtained in the experiment on a search of new resonances performed at the storage ring VEPP-2M /1/ with the detector "OLYA". The c.m. energy region 0.64-1.4 GeV was scanned with a step approximately equal to an energy spread /2/.

In Fig. 1 the lay-out of the "OLYA" detector is presented. The solid angle is 0.65 x 4π St. More detailed description of the detector is given elsewhere /2/. Note that a triggering threshold for charged kaons (C1*C2*C3) is 65 MeV. The integrated luminosity collected above this threshold is 564 nb^{-1}.

In the energy range under consideration the kaon velocity β is much less than unity. For example, at the threshold energy 1.12 GeV β = 0.47, while at the maximum energy 1.4 GeV β = 0.71. At the same time the velocity of pions coming from the reaction $e^+e^- \to \pi^+\pi^-$ is greater than 0.96. Therefore K^+K^- events are characterized by large ionization losses in scintillation counters. In Fig. 2 it is illustrated by pulse height spectra in C2 counters for kaons and electrons. For the electron spectrum experimental events selected in this experiment /3/ have been used. Kaon spectra were obtained by Monte-Carlo simulation discussed below. Even at the maximum energy kaon pulse heights are well above those for minimum ionizing particles. This very fact has been used for selection of K^+K^- events.

To study the process $e^+e^- \to K^+K^-$ events were selected with two collinear tracks coming from the interaction region:

$$|\Delta\theta| < 10^\circ, \quad |\Delta\varphi| < 10^\circ,$$

for kaons $\sigma(\Delta\theta)$ = 2.5°, $\sigma(\Delta\varphi)$ = 2°.

The fraction of K^+K^- events in the total number of detected collinear events doesn't exceed 1:100. To enhance this fraction additional cut has been imposed on the polar angle θ. For the further treatment events with $57^\circ < \theta < 123^\circ$ were taken. This decreased the detection efficiency for $e^+e^- \to e^+e^-$ by 40%, while for $e^+e^- \to K^+K^-$ - by 10% only.

The detection efficiency of K^+K^- events and pulse height spectra in scintillation counters were obtained by detailed Monte-Carlo simulation of the experiment. The simulation took into account ionization losses, multiple scattering and nuclear absorption /4/. In the pulse height simulation non-linearity of light yield at large ionization losses was included /5/. The 5% correction due to incomplite simulation of secondary processes of kaon nuclear absorption was also included in the detection efficiency.

In Fig. 3 the detection efficiency of kaon events is shown. Smooth growth of the detection efficiency is due to the increase of the kaon velocity resulting in the decrease of the number kaons decaying in front of the C3 counter or scattered at a large angle.

The energy region explored was divided in 20 MeV intervals. Events satisfying geometrical criteria were further separated in kaons and minimum ionizing particles (e^+e^-, $\mu^+\mu^-$, $\pi^+\pi^-$) by the correlation matrix method /6/. As a separation parameter the ratio of the likelihood functions for pulse heights in scintillation counters was choosen. For each particle of an event the following quantity was calculated:

$$L_i = \ln \frac{p_1(A_1) \times p_2(A_2) \times p_3(A_3)}{Q_1(A_1) \times Q_2(A_2) \times Q_3(A_3)} ,$$

where i = 1,2 is a particle number, A_1, A_2, A_3 - pulse heights in counters C1, C2, C3 normalized to the particle path length, $p_n(A_n)$ - probability to give a pulse height A_n in the n -th counter for a minimum ionizing particle, $Q_n(A_n)$ - the same probability for kaons.

The experimental spectrum of electrons from /3/ was taken as $p_n(A)$. Kaon spectra are energy-dependent and have been obtained by simulation for each 20 MeV interval separately. Figure 2 illustrates used spectra in the C2 counter for two

energy intervals.

In the energy region above 1,26 GeV kaons stop after the C5 counter. Therefore information about C4 and C5 counters was included in the separation parameter, improving separation of events at high energies.

Two-dimensional distribution L_1 by L_2 represents a correlation matrix. For example, in Fig. 4a the matrix at the maximum energy is presented. At this energy the kaon and minimum ionizing particle spectra differ the most weakly. As parameters L_1 and L_2 are calculated by pulse heights from the counters in opposite parts of the detector, the correlation between their values is due only to the fact that both detected particles are of the same type.

Therefore the number of events in each matrix cell is described by Poisson distribution with an average value

$$\overline{N}_{ij} = N_K q_i q_j + N_M p_i p_j ,$$

where N_K is a number of K^+K^- events, N_M is a number of minimum ionizing particles, q_i, p_i are probabilities to enter the i -th column (line) of the matrix.

The likelihood function was optimized in parameters N_K, N_M, q_i, p_i, i = 1,2,..., n-1, where n is a matrix dimension. As all the parameters (including q_i, p_i) were optimized, possible inaccuracies in pulse height spectra of simulated kaons influence the separation results only slightly /6/.

K^+K^- events are clearly seen both in two-dimensional hystograms and one-dimensional distributions over the sum parameter $L = L_1 + L_2$ for all energy intervals (Fig. 5).

To check the correctness of the kaon separation events with $L < -4$ have been selected (Fig. 5). This region contains 90% of all K^+K^- events, the admixture of other channels being small. Distributions of these events over the transverse distance from the beam and the polar angle Θ are presented in Fig. 6 and Fig. 7 respectively, showing good agreement with those for simulated kaons. Pulse heights spectra of selected events also exhibit coincidence with simulation.

The average velocity of the particles of these events measured by time between e^+e^- collision and C3 counter triggering varies from 0.4 to 0.7, thus confirming correct identification of kaons.

The total number of K^+K^- events obtained after data treatment is 1375. The energy distribution of kaon events is presented in Table 1. Also shown is the number of e^+e^- elastic scattering events and the integrated luminosity calculated by it /3/. Two last columns present the obtained values of the cross-section of $e^+e^- \to K^+K^-$ and kaon formfactor squared. Radiative corrections were calculated according to /7/.

In Fig. 8 obtained values of $|F_{K^+}|^2$ are shown together with the results of our previous experiment /8/. The curve is the calculation in the vector dominance model with ρ, ω, ϕ meson interference taken into account:

$$F_{K^+} = \frac{1}{2}\frac{m_\rho^2}{\Delta_\rho} + \left(\frac{1}{2} - \frac{f_{\phi K\bar{K}}}{f_\phi}\right)\frac{m_\omega^2}{\Delta_\omega} + \frac{f_{\phi K\bar{K}}}{f_\phi}\frac{m_\phi^2}{\Delta_\phi} \quad (1)$$

where $\Delta_V = m_V^2 - s - i m_V \Gamma_V$ and for ϕ - meson coupling constants the experimental value is taken /9,10/:

$$\frac{f_{\phi K\bar{K}}}{f_\phi} = 0.33 .$$

For simplicity finite width corrections are omitted, that results in a 10% inaccuracy in the calculated value of the formfactor.

In the whole explored energy region experimental values of $|F_{K^+}|$ exceed considerably the predictions of the vector dominance model based on ρ, ω, ϕ - mesons. At the maximum energy the ratio of the experimental to theoretical values is three.

Note that a similar effect–excess of experimental values

T a b l e 1

2E, Gev	$N_{e^+e^-}$	$\mathcal{L}_{e^+e^-}$, nb^{-1}	$N_{K^+K^-}$	Total cross section nb	$\lvert F_{K^+}\rvert^2$
I.I2-I.I4	I0697+I05	30.4	48.6+ 7.0	I0.30+2.65	5.26+I.35
I.I4-I.I6	9700+I28	28.5	69.I+ 9.0	8.87+I.40	4.0I+0.63
I.I6-I.I8	93I3+ 98	28.4	74.6+ 9.0	8.26+I.I3	3.37+0.46
I.I8-I.20	I0852+I05	34.3	99.3+I0.0	8.47+0.95	3.I7+0.36
I.20-I.22	I6696+I04	35.0	66.9+ 8.5	5.38+0.73	I.88+0.26
I.22-I.24	I0277+I0I	34.7	83.6+ 9.5	6.68+0.83	2.I9+0.27
I.24-I.26	I04I9+I03	36.3	83.6+ 9.5	6.28+0.78	I.96+0.24
I.26-I.28	I2897+II4	46.4	I27.4+I2.0	7.37+0.79	2.20+0.24
I.28-I.30	II438+I07	42.5	98.8+II.0	6.I7+0.77	I.77+0.22
I.30-I.32	II245+I06	43.I	II6.0+I9.0	7.06+I.22	I.97+0.34
I.32-I.34	I0934+I05	43.2	I04.3+I4.0	6.24+0.90	I.69+0.24
I.34-I.36	I2838+II3	52.3	I34.5+I2.0	6.57+0.68	I.74+0.I8
I.36-I.38	II9I7+I09	50.0	I27.8+I2.0	6.4I+0.68	I.66+0.I8
I.38-I.40	I3566+II7	58.6	I4I.0+I4.0	5.69+0.63	I.45+0.I6

over theoretical predictions is observed in the reaction $e^+e^- \to \pi^+\pi^-$ as well /3/. According to the modern conceptions this is due to the effect of inelastic channels /11,12/. However, the assumption that inelastic channels give the same contribution to the isovector part of the kaon formfactor, doesn't provide the quantitative explanation of the excess observed. It is clear that for better understanding of the situation measurement of a neutral kaon formfactor is needed. Knowledge of both F_{K^+} and F_{K^0} allows to separate the isoscalar and isovector parts of the kaon formfactor.

In Fig. 9 we present all available information on $|F_{K^+}|^2$ in the energy region from 1.0 up to 2.2 GeV. Note that recent results from DCI /13/ also indicate to a considerable excess of $|F_{K^+}|^2$ over vector dominance predictions at $2E \sim 1.6$ GeV.

If one considers the energy behaviour of $|F_{K^+}|^2$ as the resonant one, then for simultaneous description of the $|F_{K^0}|^2$ smallness /13/ two new resonances have to be postulated (isovector and isoscalar). Only in this case the interference with ρ, ω, φ - meson tails can result in an increase of $|F_{K^+}|^2$ without similar increase of $|F_{K^0}|^2$.

Such a possibility was discussed in /14,15/ where four-quark resonances (molecules) had been predicted with a mass about 1.5 GeV. As shown in /15/, the crucial test of this model is provided by the observation of $\varphi\pi$ decay of the new resonance. Note that the fit (two-resonance) of both our and DCI data allows satisfactory description of the kaon formfactor behaviour. However, further information on K^+ and K^0 formfactor is badly needed to elucidate the picture. At the moment the presented considerations seem a bit too speculative.

In conclusion the authors express their profound gratitude to the whole staff of VEPP-2M who ensured excellent performance of the accelerator. Thanks are also due V.M.Budnev, E.V.Shuryak and A.I.Vainshtein for numerous fruitful discussions.

References

1. G.M.Tumaikin, Proceedings of the 10 International Conference on High Energy Accelerators, Serpukhov, 1977, vol. 1, p. 443.
2. V.M.Aulchenko et al., Preprint INP 79-65, Novosibirsk, 1979.
3. I.A.Koop et al., Preprint INP 79-67, Novosibirsk, 1979.
4. A.D.Bukin, S.I.Eidelman, Preprint INP 77-101, Novosibirsk, 1977.
5. R.L.Craun and D.L.Smith, Nucl. Instr. and Meth. 80 (1970) 239.
6. A.D.Bukin et al., Preprint INP 77-92, Novosibirsk, 1977.
7. S.I.Eidelman and E.A.Kuraev, Phys. Letters 80B (1978) 94.
8. V.A.Sidorov, Proceedings of the 18 International Conference on High Energy Physics, Vol. 2, p. B13, Tbilisi, 1976.
9. J.C.Bizot et al., Phys. Letters 32B (1970) 416.
10. V.E.Balakin et al., Phys. Letters 34B (1971) 328.
11. V.N.Baier and V.S.Fadin, Pisma v JETF 15 (1972) 219.
12. N.M.Budnev et al., Phys. Letters 70B (1977) 365.
13. J.C.Bizot et al., Report at the International Conference on High Energy Physics, Geneve, 1979.
14. R.L.Jaffe, Phys. Rev. D 15 (1977) 267, 281.
15. F.E.Close and H.J.Lipkin, Phys. Rev. Lett. 41 (1978) 1263.
16. V.E.Balakin et al., Phys. Letters 41B (1972) 205.
17. M.Bernardini et al., Phys. Letters 46B (1973) 261.
18. D.Bollini et al., Lett Nuovo Cim. 14 (1975) 418.
19. B.Esposito et al., Phys. Letters 67B (1977) 239.

Fig. 1. Detector "OLYA"

Fig. 2. Pulse height spectra of kaons and electrons in the C2 counter: kaons-simulation, electrons - experiment /3/.

Fig. 3. Energy dependence of the detection efficiency of K^+K^- events.

Fig. 4. Correlation matrices:
a) For the maximum energy, where separation of K^+K^- events is the most difficult. Kaon events concentrate in the left upper corner, minimum ionizing particle events - in the right lower one.
b) For the energy below the triggering threshold (to illustrate the absence of background).

Fig. 5. Distributions in the sum separation parameter $L = L_1 + L_2$.

Fig. 6. Distribution of separated K^+K^- events in the transverse distance from the beam:
hystogram - simulation,
points - experiment.

Fig. 7. Distribution of separated K^+K^- events in the polar angle : hystogram - simulation, points - experiment.

Fig. 8. Energy dependence of the charged kaon formfactor. The curve is the prediction of vector dominance with ρ, ω and ϕ - mesons (formula (1)).

Fig. 9. All data available on $|F_{K^+}|^2$ in the energy range $1 < 2E < 2.2$ GeV. The curve is the prediction of vector dominance with ρ, ω and ϕ - mesons (formula(1)).

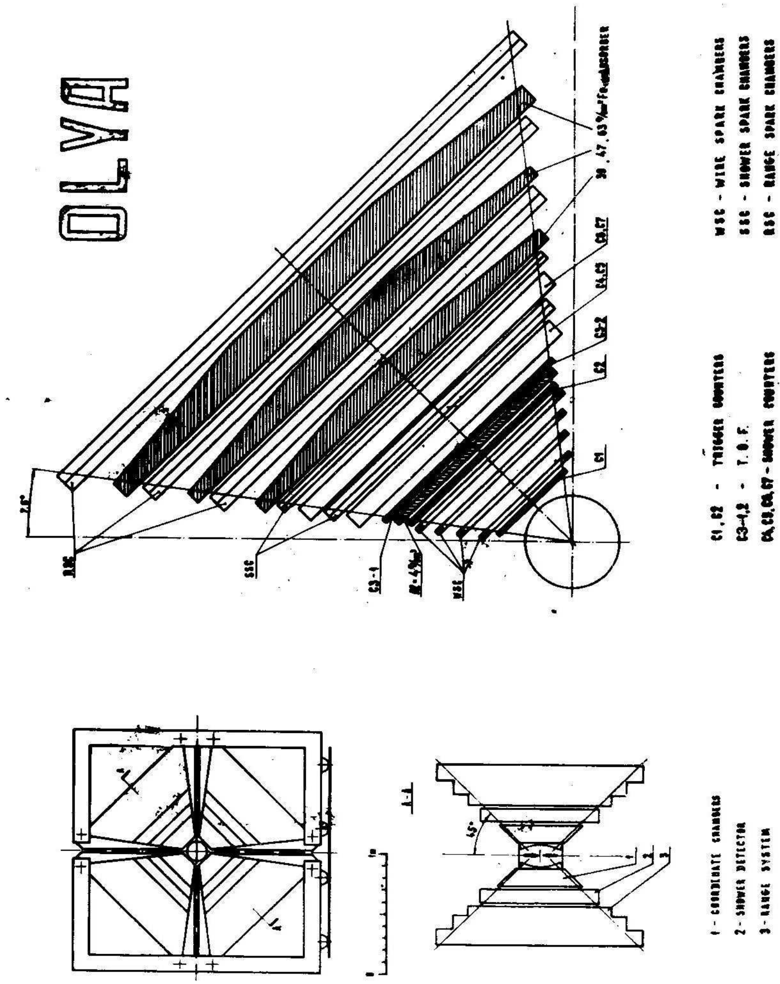

Fig. 1

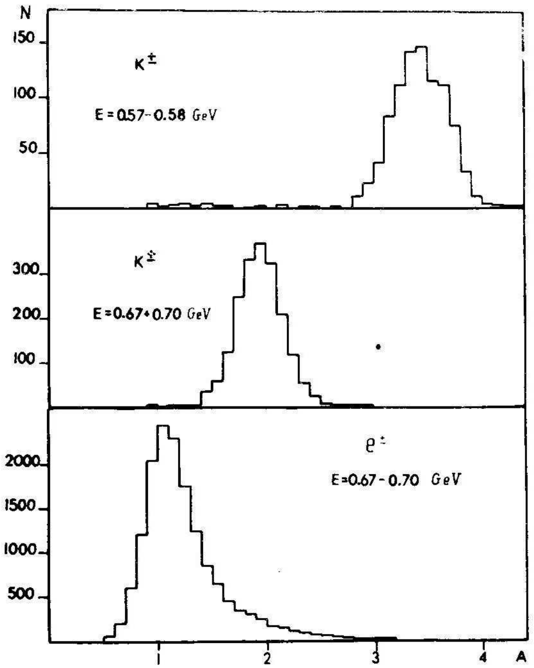
N
150
100
50
K±
E = 0.57–0.58 GeV
300
200
100
K±
E = 0.67÷0.70 GeV
2000
1500
1000
500
e±
E = 0.67 - 0.70 GeV
1
2
3
4
A

Fig. 2

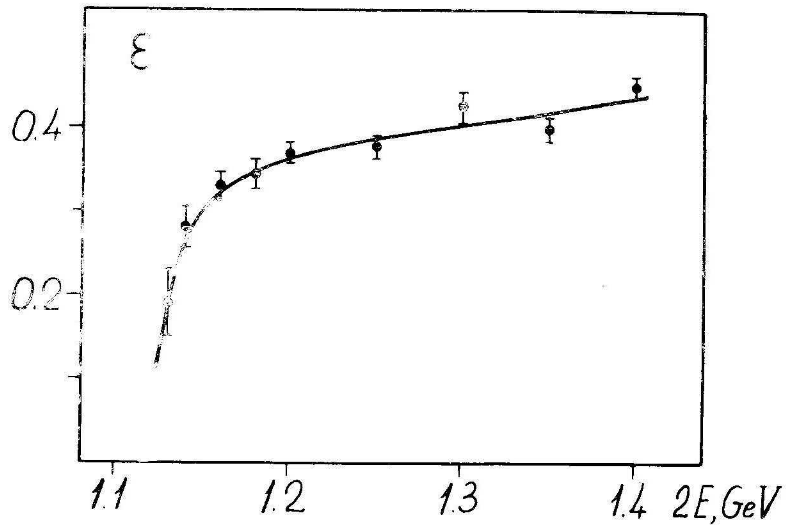
ε
0.4
0.2
1.1
1.2
1.3
1.4
2E, GeV

Fig. 3

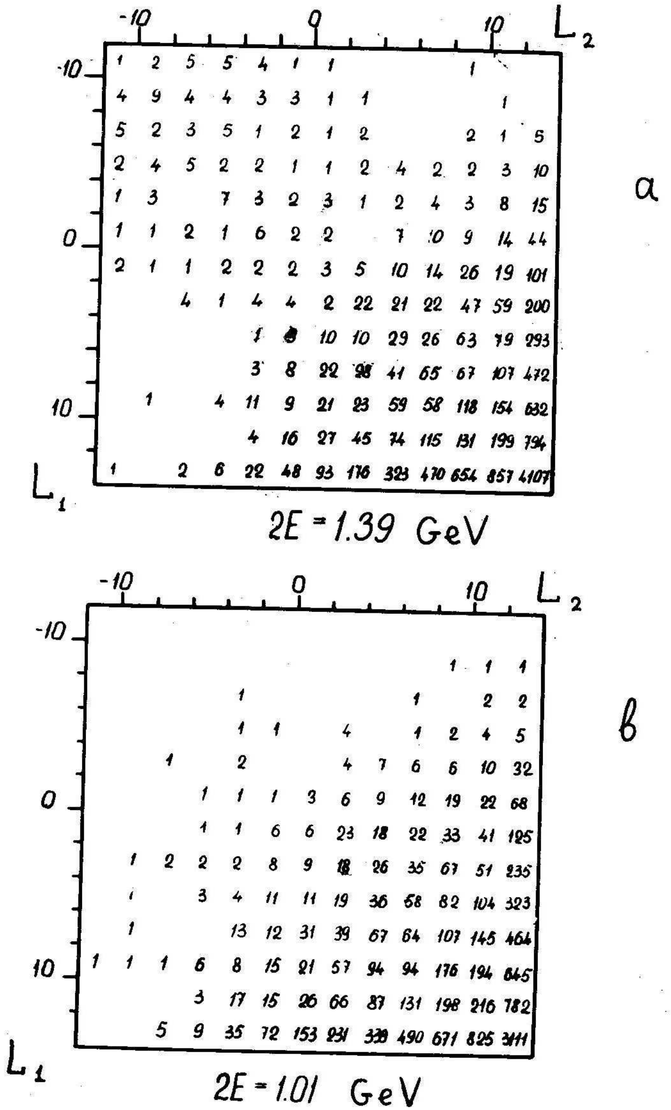

L_2
L_1
-10
0
10
a
2E = 1.39 GeV
b
2E = 1.01 GeV

Fig. 4

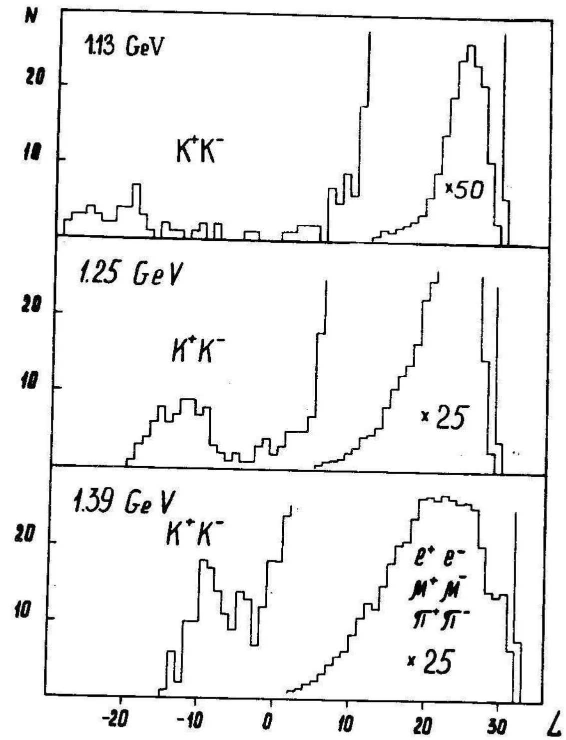

N
1.13 GeV
K^+K^-
×50
1.25 GeV
K^+K^-
×25
1.39 GeV
K^+K^-
e^+e^-
$\mu^+\mu^-$
$\pi^+\pi^-$
×25
-20
-10
0
10
20
30
L

Fig. 5

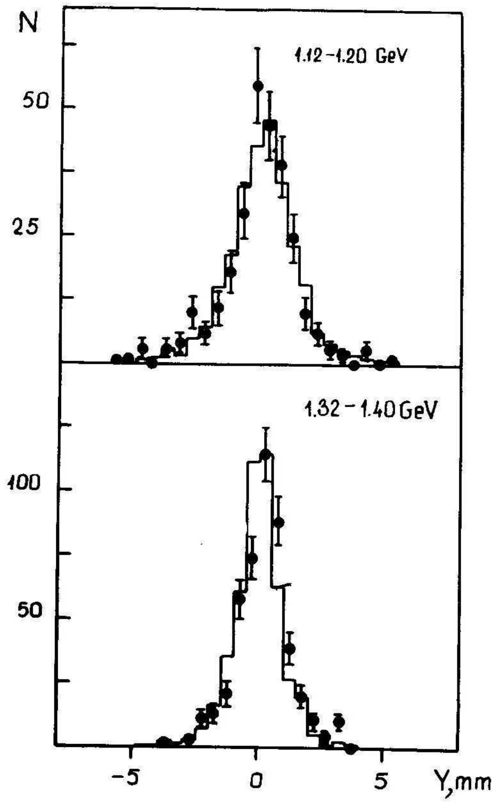
N
50
25
1.12–1.20 GeV
100
50
1.32–1.40 GeV
-5
0
5
Y,mm

Fig. 6

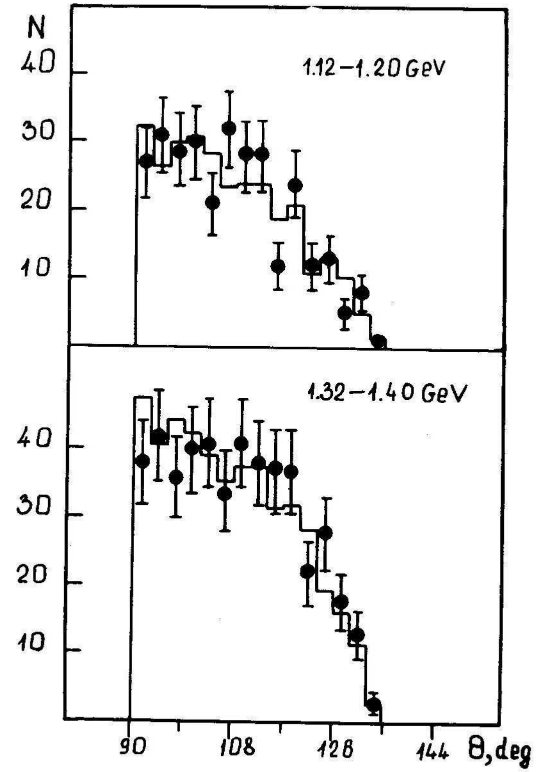
N
40
30
20
10
1.12–1.20 GeV
40
30
20
10
1.32–1.40 GeV
90
108
128
144
θ,deg

Fig. 7

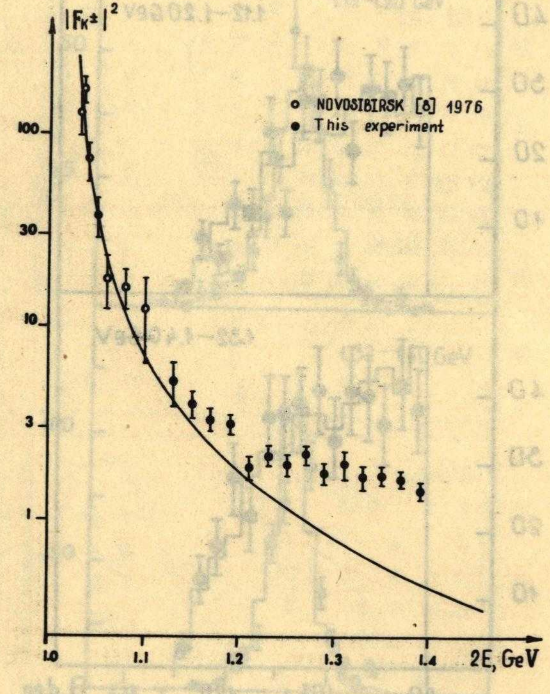

|Fk±|²
NOVOSIBIRSK [8] 1976
This experiment
100
30
10
3
1
1.0
1.1
1.2
1.3
1.4
2E, GeV

Fig. 8

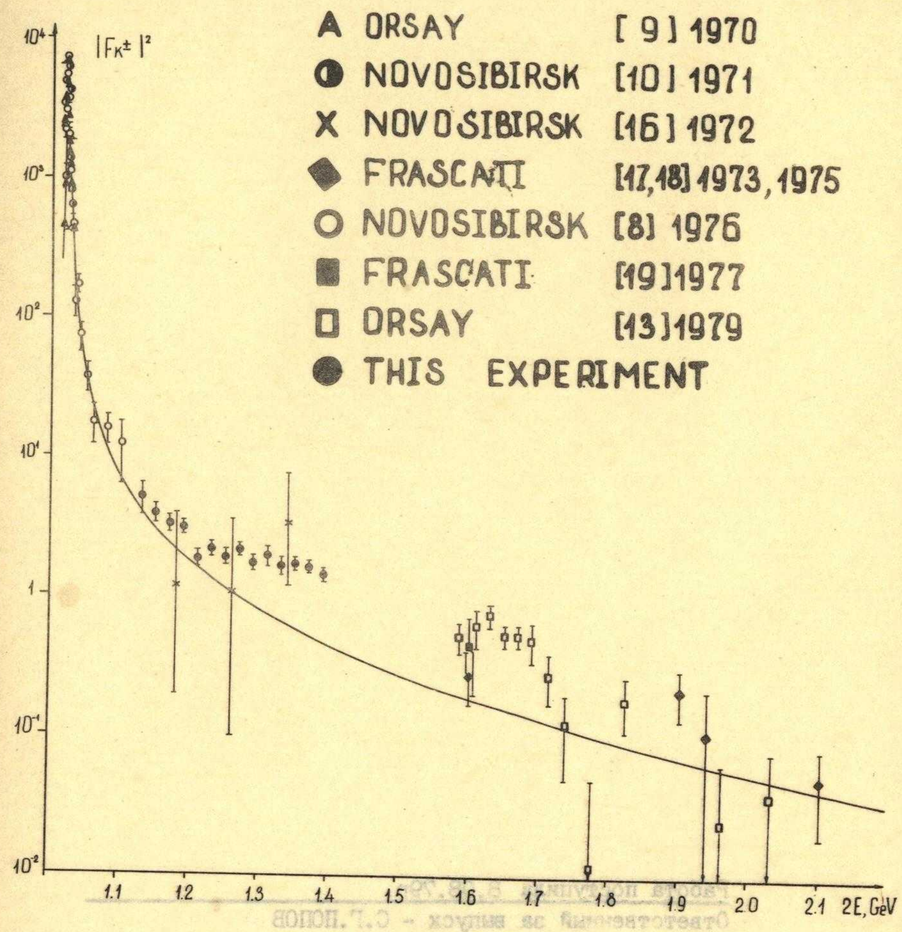

|Fk±|²
ORSAY [9] 1970
NOVOSIBIRSK [10] 1971
NOVOSIBIRSK [16] 1972
FRASCATI [17,18] 1973, 1975
NOVOSIBIRSK [8] 1976
FRASCATI [19] 1977
ORSAY [13] 1979
THIS EXPERIMENT
1.1
1.2
1.3
1.4
1.5
1.6
1.7
1.8
1.9
2.0
2.1
2E, GeV

Fig. 9

Работа поступила 8.08.79г.

Ответственный за выпуск - С.Г.ПОПОВ
Подписано к печати I5.08.79г. МН 02975
Усл. I,3 печ.л., I,I учетно-изд.л.
Тираж 200 экз. Бесплатно.
Заказ №68

Отпечатано на ротапринте ИЯФ СО АН СССР